

Temperature and salinity extremes from 2014-2019 in the California Current System and its source waters

Alice S. Ren ¹✉ & Daniel L. Rudnick ¹

The California Current System in the eastern North Pacific Ocean has experienced record high temperatures since the marine heatwave of 2014-2016. Here we show, through a compilation of data from shipboard hydrography, ocean gliders, and the Argo floats, that a high-salinity anomaly affected the California Current System from 2017-2019 in addition to the anomalously high temperatures. The salinity anomaly formed in 2015 in the North Pacific Subtropical Gyre and was subsequently advected into the California Current System, in a generation mechanism different from the events leading to the marine heatwaves of 2013/2014 and 2019 in the North Pacific. The salinity anomaly was unique in at least 16 years with an annual mean deviation from the long-term average greater than 0.2 and anomalies greater than 0.7 observed offshore. Our results imply that different source waters were found in the California Current from 2017-2019, with the near-surface California Current salinity rivaling that of the California Undercurrent.

¹Scripps Institution of Oceanography, La Jolla, CA, USA. ✉email: aren@ucsd.edu

The California Current System (CCS) is the eastern boundary current system in the North Pacific. The CCS consists of an equatorward-flowing, surface-intensified current, the California Current, and a subsurface-intensified, poleward-flowing current, the California Undercurrent. These mean currents are accompanied by numerous eddying features and an annual cycle including wind-driven upwelling. The coastal environment of the central and southern CCS has experienced anomalously high-temperature conditions since 2014 (refs. 1–4). The high-temperature anomaly began in 2014 with the marine heatwave (MHW) that affected the central and southern CCS⁵. Positive temperature anomalies in the surface 50 m of the CCS during 2014–2015 were above 4 °C⁵. We document changes in temperature and salinity that are unique to the time period 2014–2019, expanding on previous studies that have focused on temperature alone. In particular, we document a salinity anomaly that affected the CCS from 2017 to 2019 but formed offshore in 2015. The salinity anomaly was noted in the annual report describing the physical and biological condition of the CCS organized and published by the California Cooperative Oceanic Fisheries Investigations (CalCOFI).^{2,6} The relevance of regional salinity changes is that they often indicate changes of source water which may have a large impact on the marine ecosystem.

During the time period from 2014 to 2019, some established relationships between sea surface temperature (SST) or SST indices and biological indicators reversed, diverging from patterns established up to 2010. Before the onset of the 2014–2016 MHW, fluctuations in sardine and anchovy were largely believed to be related to SST^{7–10} with higher sardine populations under warm conditions and higher anchovy populations under cool conditions, though there were alternate hypotheses^{11–13}. The abundance of salmon was similarly correlated with a large-scale index of SST, the Pacific Decadal Oscillation (PDO)¹⁴. In 2016–2017 northern anchovy was found in high abundance during high SST off central and southern California while Pacific sardine abundance was relatively low^{15,16}, opposite to the relationship established from 1950 to 2002 (ref. 7). Subsequently, in 2019, northern anchovy were abundant throughout the CCS while Pacific sardine were locally abundant off central California². This is similar to findings in the Gulf of Alaska from 2014 to 2019, a period of rapid ocean warming, where the relationship between the PDO and salmon abundance switched from a positive or neutral correlation to a negative correlation¹⁷. The implication is that previously established correlations of biological abundance with large-scale SST indices did not have predictive power during the MHW of 2014–2016 and its aftermath¹⁸. In contrast, from 1983 to 2016 young of the year (YOY) rockfish abundance was found to be related to salinity on the isopycnal 26.0 kg m⁻³, interpreted to be an indicator of changes in the water mass composition of the CCS¹⁹. Here, we examine the temperature and salinity record to identify changes in the physical environment.

Results and discussion

The temperature record from the southern California Current at 10 m (Fig. 1a) from the CalCOFI and California Underwater Glider Network (CUGN) demonstrates the unusually high-temperature event in 2014–2016 (Fig. 1b). The temperature in 2015 was the highest in the California Current based on the time series of almost 70 years. The 1997/1998 El Niño event does not show up strongly in the time series at 10 m because larger anomalies in temperature were observed at depth and inshore due to the influence of the California Undercurrent and thermocline displacement^{20,21}. The extreme in temperature in 2015 is followed by cooler conditions, but from 2016 to 2019, the California Current was still warmer than the baseline, here taken as the

mean of years 2007–2013 (see “Methods” for details). The 2007–2013 baseline is chosen for all three datasets used in this manuscript: CalCOFI, CUGN, and Argo. The CalCOFI 2007–2013 time period is 0.55 °C cooler and 0.010 fresher than the often-reported CalCOFI baseline of 1984–2012 and 0.33 °C cooler and 0.037 fresher than the full time series from 1950 to 2019 here. There is discussion in the literature of two separate MHWs with different generation mechanisms in the Northeast Pacific, one beginning in the winter of 2013/2014 (ref. 22) and one beginning in the summer of 2019 (ref. 23); however, the southern CCS has had one extended period of elevated temperatures. The CUGN and CalCOFI temperature anomaly time series agree well during the MHW from 2014 to 2016, while they agree within the 99% confidence interval of the CalCOFI time series in the times before and after.

From 2017 to 2019, in addition to a warm temperature anomaly, the CCS experienced a high-salinity anomaly. The salinity anomaly, identified offshore at 10 m from CUGN and CalCOFI observations on Lines 80.0 and 90.0, had an annual anomaly approaching 0.3 in 2018 (Fig. 1c). The 2017–2019 salinity anomaly was the strongest on record in this region since 2001. The period since 2003 was one of relative low salinity, gradually increasing with small interannual fluctuations. The 2017–2019 salinity anomaly was the culmination of this 15-year period of increasing salinity. The CUGN and CalCOFI salinity anomaly time series match remarkably well.

Hovmöller diagrams of depth-averaged salinity anomaly from 10 to 100 m from CUGN gliders (Fig. 2a–c) show how the 2017–2019 salinity anomaly approached the coast. The 10–100 m depth range was chosen to focus on the surface mixed layer and to avoid the halocline that exists in the mean from 105 to 135 m depth in the offshore portions of Lines 66.7, 80.0, and 90.0 examined here (Supplementary Fig. 1). Salinity anomalies plotted against depth near the region of the halocline are often caused by isopycnal heave. The salinity anomaly began in early 2017 on transect Line 66.7 (for location see Fig. 1a) and in middle and late 2017 on Lines 80.0 and 90.0, respectively. The salinity anomaly was stronger offshore and appeared to pass through the northern line, Line 66.7, before the southern lines, Line 80.0 and Line 90.0. The high-salinity anomaly ended on Line 66.7 in the middle of 2019 while continuing through the end of 2019 on Lines 80.0 and 90.0. Peak salinity anomalies averaged from 10 to 100 m reached a maximum of 0.6 on each of the three lines. Plots of salinity anomaly over depth and time, averaged over the distance between stations 70 and 100 of the CalCOFI grid, demonstrate that the salinity anomaly was largest in the top 100 m (Fig. 2d–f). Due to high-salinity anomalies that occurred first on the offshore edge on Line 66.7 and that did not dominate the across-shore average, the salinity anomaly begins at near the same time on all three lines when viewed from the depth versus time perspective.

Hovmöller diagrams of depth-averaged temperature anomaly from 10 to 100 m show the salinity anomaly in contrast with the anomalous warmth from 2014 through the end of 2019 on all three lines (Fig. 3a–c). The 10–100 m depth-averaged temperature anomaly during 2014–2019 was frequently greater than 3 °C and exceeded 4 °C on Lines 66.7 and 90.0, while it approached 4 °C on Line 80.0. The temperature anomaly was also concentrated in the top 100 m (Fig. 3d–f) as seen from plots of temperature anomaly over depth and time, averaged over the distance between stations 70 and 100 of the CalCOFI grid. The across-shore averaged plots show that the high-temperature anomaly remained in the central and southern CCS after 2016 and until 2019.

The origin of the salinity anomaly is examined in the greater Pacific Ocean. Basin-wide salinity anomalies at 10 db from the Roemmich–Gilson (R–G) climatology of Argo float data²⁴ demonstrate that the anomaly originated offshore in September

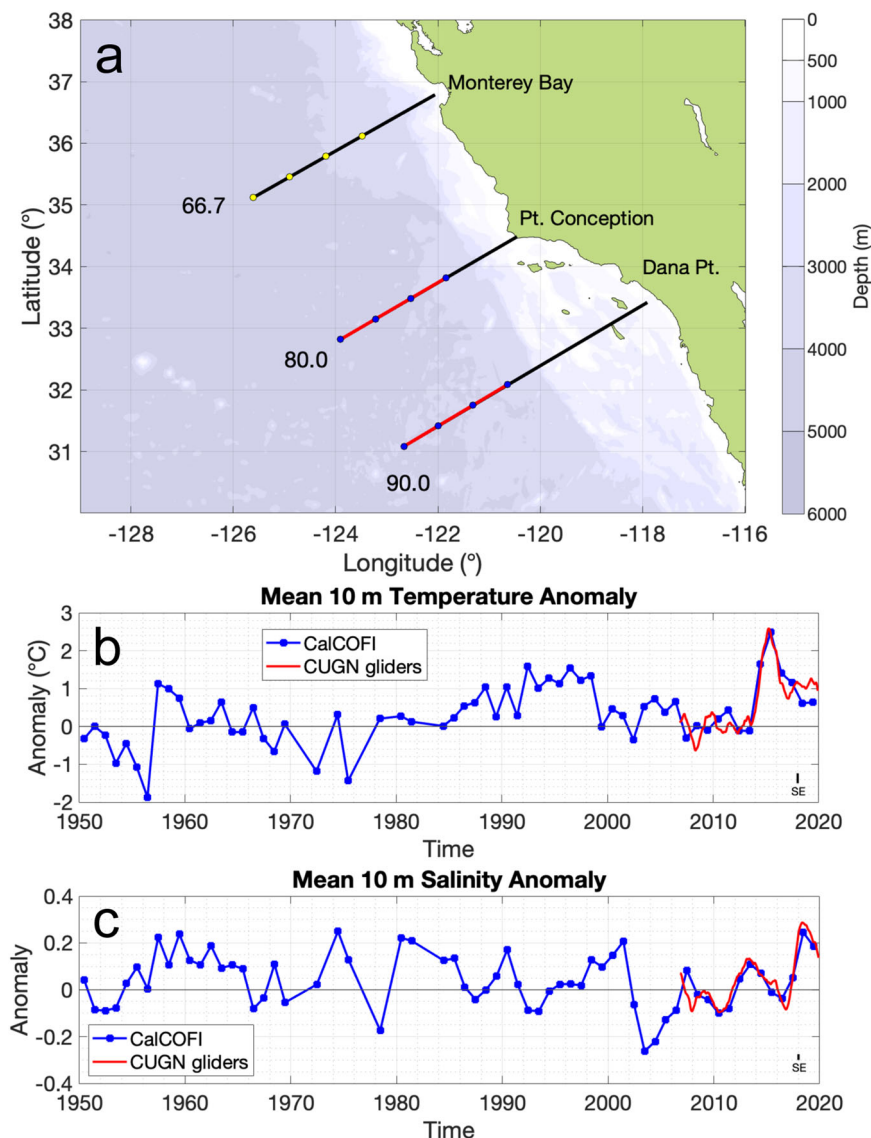


Fig. 1 Historical offshore temperature and salinity observations in the California Current. **a** Location of the CUGN glider Lines 66.7, 80.0, and 90.0 (black). The location of the portions of Line 80.0 and Line 90.0 of the CUGN glider lines used in the time series is overplotted in red while CalCOFI stations 70, 80, 90, and 100 along Lines 80.0 and Lines 90.0 used in the time series are plotted in blue dots. Stations 70, 80, 90, and 100 of Line 66.7 are plotted in yellow dots. **b** The 10 m annual mean temperature anomaly (°C) from CalCOFI (blue) and 365-day lowpass filtered temperature anomaly (°C) from CUGN (red). **c** The 10 m annual mean salinity anomaly from CalCOFI (blue) and 365-day lowpass filtered salinity anomaly from CUGN (red). The CalCOFI average is calculated from stations 70, 80, 90, and 100 on Lines 80.0 and 90.0 while the CUGN average is from the distance between stations 70 and 100 on Lines 80.0 and 90.0. The average annual standard error of the CalCOFI temperature anomaly (0.26 °C) and salinity anomaly (0.025) is plotted as a black bar in the lower right-hand corner in **b** and **c**, respectively.

2015, years before its detection along the California coast (Fig. 4). In the 8-month interval plots, the anomaly appears in September 2015 and then follows the path of the surface geopotential height contours east towards the coast and then south towards the equator. The plotted monthly surface geopotential height contours are approximate streamlines of the ocean currents and indicate the portion of the North Pacific Current that feeds into the California Current and the southward limb of the North Pacific Subtropical Gyre. While a pattern of positive salinity anomaly between 160° and 170°W at 40°N also occurred in the Argo data in 2010–2011, 2017–2019 was the only instance in the Argo record (2004–2019) when an anomaly persisted, intensified, and subsequently moved equatorward along the coast. The persistence of the salinity anomaly from 2015 to at least 2019 in the eastern North Pacific is unique in the Argo record.

The salinity anomaly had a large spatial extent not measured by the coastal CUGN lines or CalCOFI hydrography but captured by Argo. The salinity anomaly was quite strong offshore; in September 2017, the positive salinity anomaly at 35.5°N, 135.5°W was 0.78. The edge of CUGN Line 66.7, corresponding to station 100 on the CalCOFI grid, is 35.5°N 125.5°W, which is usually well approximated by the location of the 1951 m geopotential height contour. Considering the plots of May 2016 and January 2017, the salinity anomaly existed offshore but did not reach the edge of the CUGN lines. This is consistent with CUGN observations that only showed a strong salinity anomaly after January 2017 on Line 66.7 and June 2017 on Lines 80.0 and 90.0. In addition, not of primary interest in this paper, but readily apparent, is an extremely strong fresh salinity anomaly that formed to the west of the salinity anomaly and also appears to be advecting eastward in the

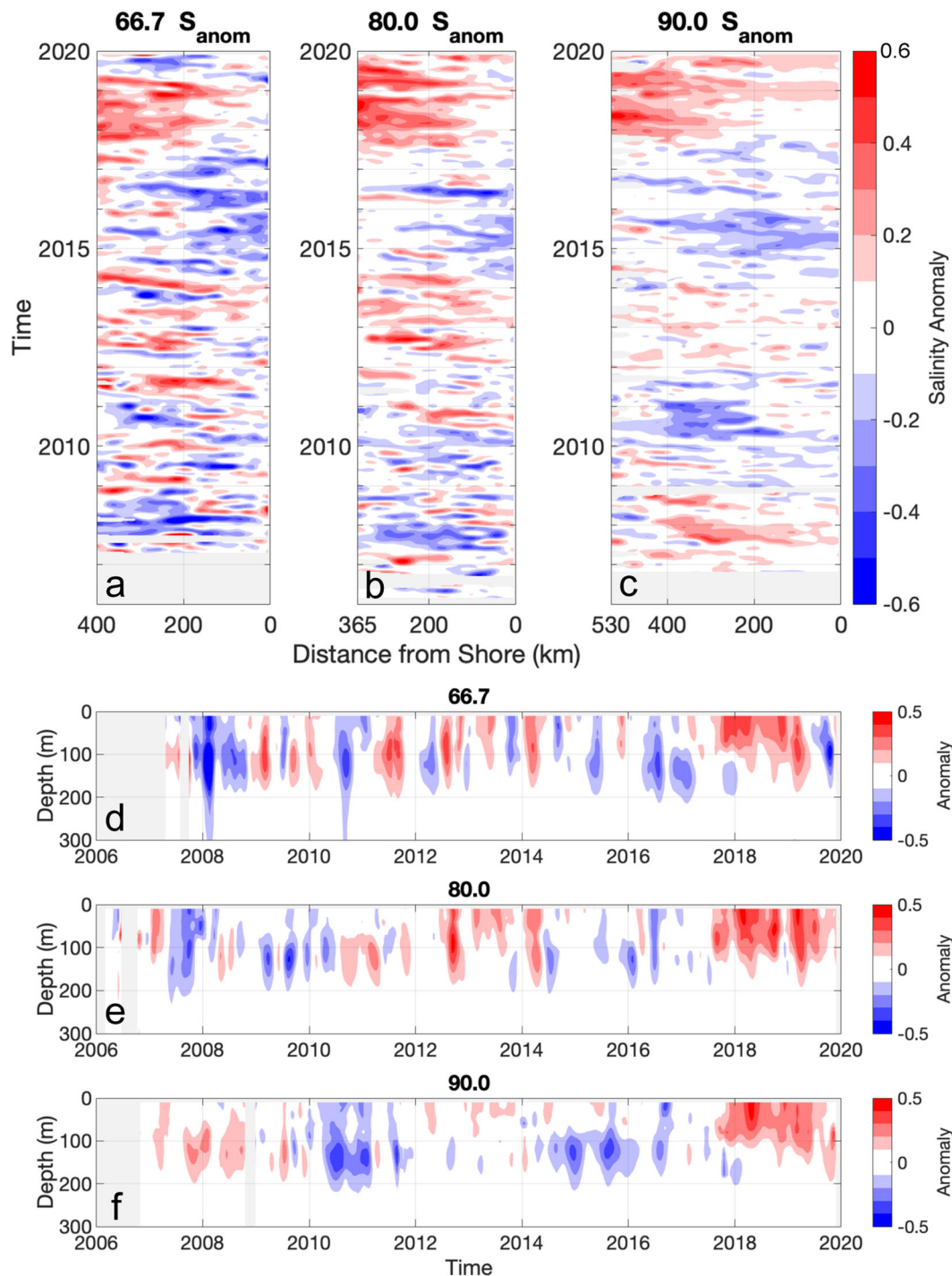


Fig. 2 Hovmöller diagrams of salinity anomaly from CUGN gliders on Lines 66.7, 80.0, and 90.0. **a–c** 10–100 m depth-averaged salinity anomaly on each of the respective lines and **d–f** spatially averaged salinity anomaly from the distance between CalCOFI stations 70–100 on each of the respective lines.

North Pacific Current as of 2019. It is possible that this fresh anomaly will appear in the CCS in coming years.

Possible causes of the salinity anomaly include advection, surface fluxes by precipitation and evaporation (E–P), and vertical turbulent entrainment. From the Argo and CUGN data, we suggest that one important factor is advection. The eastward salt flux by the North Pacific Current in the surface 100 m across 135° W from 35–44°N (Fig. 5a) was calculated and shows a large positive anomaly which begins in the second half of 2016, peaks in 2017, and ends in mid-2018. This matches the timing of the positive salinity anomalies that moved through the region

according to the salinity anomaly plots at 10 db (Fig. 4) and provides strong evidence that the salinity anomaly was advected east into the region where the California Current begins. Along CUGN lines, an increased southward advection of salt is not clear; however, even though the mean salinity, as averaged over the top 100 m and over the entire lines, increases in 2017–2019 (Fig. 5b, c). Here, southward velocities are treated as positive so consequently a positive value indicates southward advection. From 2017 to 2019, the salt flux is positive on all three lines indicating the mean flow was southward, consistent with the presence of the California Current. The alongshore salt flux may

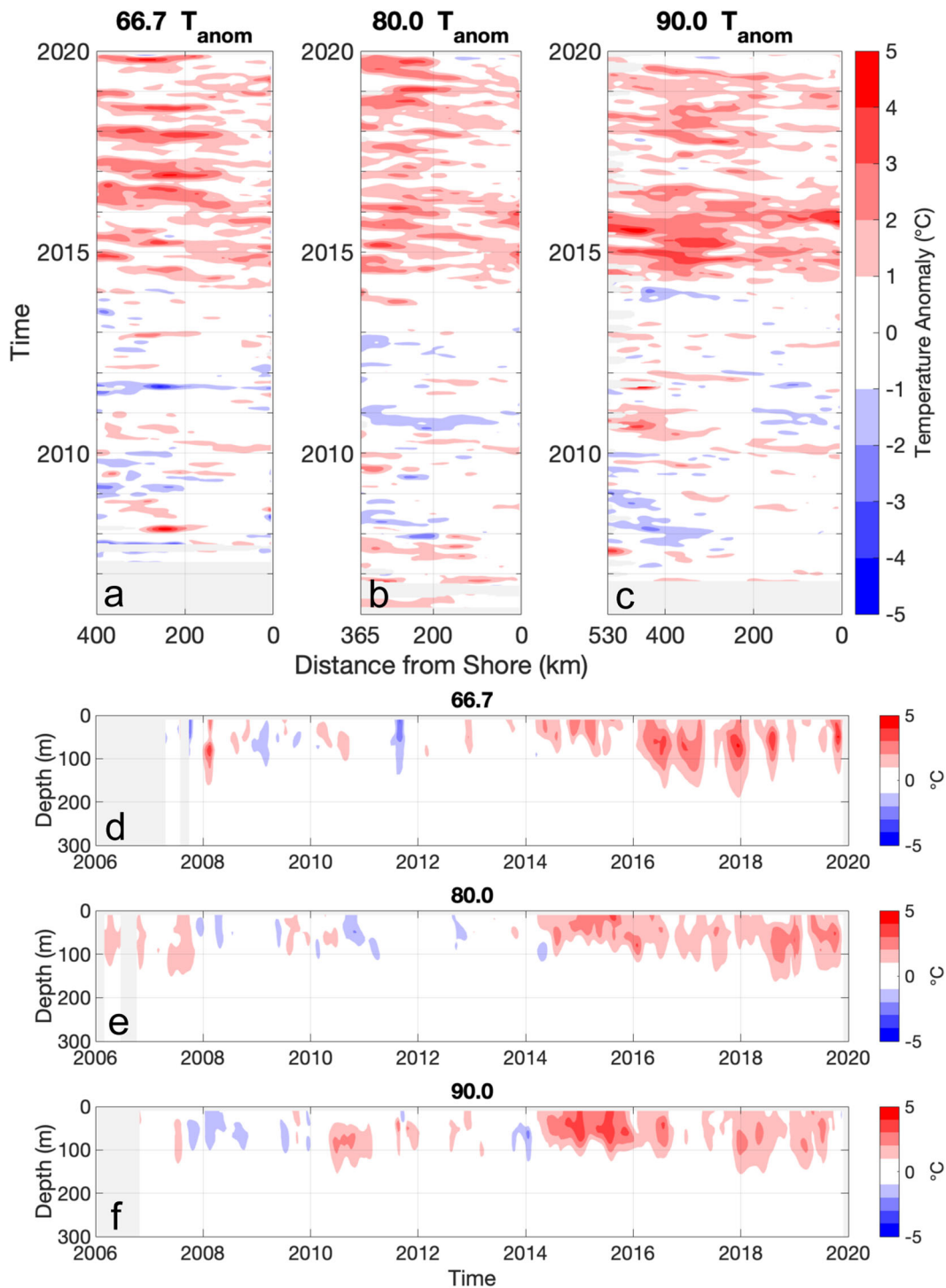


Fig. 3 Hovmöller diagrams of temperature anomaly (°C) from CUGN gliders on Lines 66.7, 80.0, and 90.0. a-c 10–100 m depth-averaged temperature anomaly on each of the respective lines and **d-f** spatially averaged temperature anomaly from the distance between CalCOFI stations 70–100 on each of the respective lines.

be difficult to measure in an eddying environment like in the CCS. The salinity anomaly of 2017–2019 was roughly 0.2 compared to a mean of 33.3. In contrast, the standard deviation of the alongshore geostrophic velocity was 0.03 m s^{-1} compared to a mean geostrophic velocity of 0.02 m s^{-1} southward (over the entire lines 66.7, 80.0, and 90.0), emphasizing the eddying nature of the CCS. Thus, changes in salt flux were dominated by changes in volume flux in the CUGN region. There is also possibly an onshore component, as suggested from the Argo salinity anomaly

plots (Fig. 4). A more complete analysis of the causes of the salinity anomaly may require an assimilative ocean circulation model.

From 2013 to 2019, it is apparent that numerous environmental forcing mechanisms were abnormal in the North Pacific. The winter 2013/2014 MHW in the North Pacific is thought to be due to changes in ocean advection and reduced heat loss from the ocean to the atmosphere²². The extension of the MHW through 2016 and transformation into a coastal SST pattern may rely on

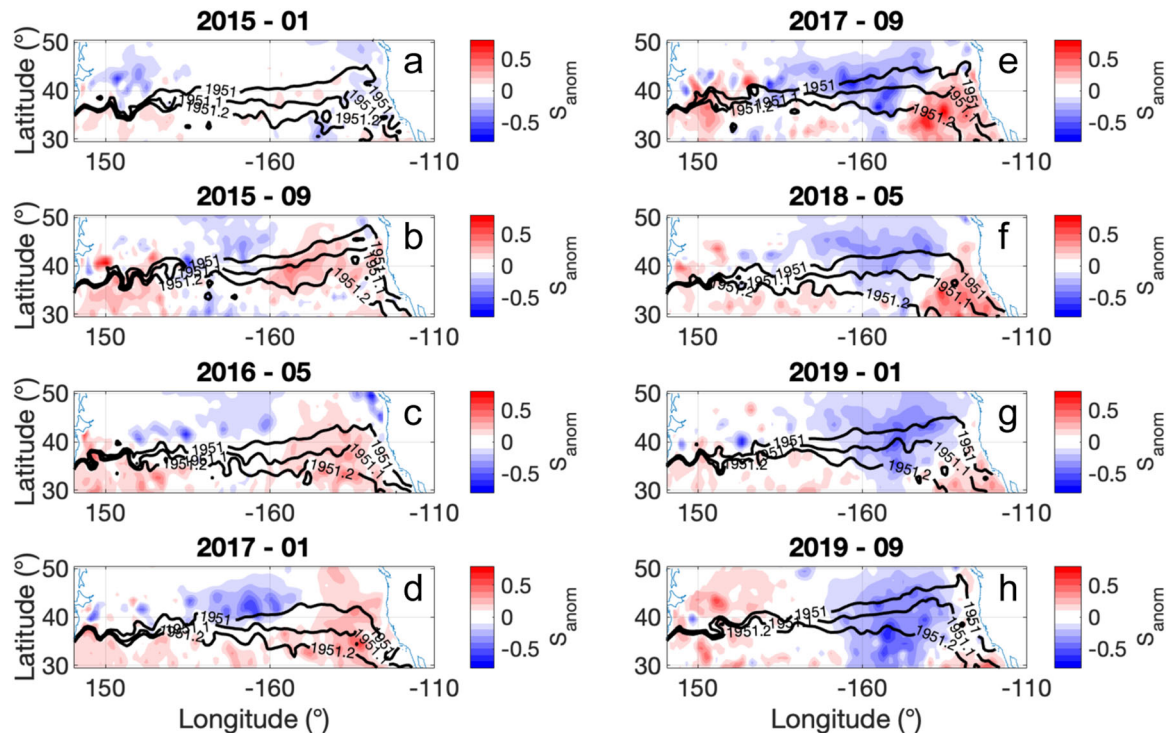


Fig. 4 Plots of salinity anomaly at 10 db from the R-G Argo climatology. Plots are in 8-month intervals including **a** January 2015, **b** September 2015, **c** May 2016, **d** January 2017, **e** September 2017, **f** May 2018, **g** January 2019, and **h** September 2019. The geopotential height (m) of select contours of the North Pacific Current that contribute to California Current and southward limb of the North Pacific Subtropical Gyre are overplotted for each month. Notice that the aspect ratio of degrees latitude to degrees longitude has been stretched in the latitudinal direction to better show characteristics of the salinity anomaly.

complex interactions between the ocean and atmosphere²⁵ while its extension through 2019 remains to be explained. Local mechanisms in the CCS during 2014–2016 include increased heat flux from the atmosphere and increased heat flux from horizontal and vertical advection⁴. The summer 2019 MHW in the North Pacific is thought have formed due to increased short wave radiation on the surface ocean and reduced surface winds, which reduced heat loss from the ocean to the atmosphere and reduced mixing and entrainment²³. While the salinity anomaly advected into the source waters of the California Current, the possible causes for the salinity anomaly's formation in 2015 in the central North Pacific are increased evaporation, increased entrainment from below, or advection of saltier water from further south in the subtropical gyre.

The salinity anomaly was not predicted by the North Pacific Gyre Oscillation (NPGO), a climate index thought to be relevant to salinity in the CCS. The NPGO, the second EOF of sea surface height anomaly in the North Pacific, was in a strongly negative phase from October 2017 to at least June 2019 (ref. ²), and the negative phase, or phase with reduced sea surface height anomaly difference between the Alaska Gyre and the North Pacific Subtropical Gyre, has been associated with fresh, or negative, sea surface salinity anomalies²⁶. In particular, the positive (negative) phase of the NPGO was correlated with greater (less) upwelling in the past which was the explanation for why salinity and other variables were related to the NPGO²⁶. One explanation is that the causal mechanism that linked CCS salinity to the NPGO may have changed^{6,27}. Another is that the relationship between salinity and the NPGO was based on relatively short records and may not hold as longer climate records are collected.

The California Current is usually the source of fresher water into the CCS, and yet in 2017–2019, it was a source of salty water that spread from offshore towards the coast. The values of salinity

in the California Current in 2018 rival values in the California Undercurrent at the surface (Fig. 6), especially on Line 90.0. From the temperature and salinity (T - S) diagrams, it is clear that the surface temperature in 2018 was warmer than the mean both inshore (0–100 km) and offshore (200–400 km) while the surface salinity was significantly saltier offshore (200–400 km). Figure 6 shows the top sections of curves in 2018 (dashed red for offshore, dashed blue for inshore) are located further up (warmer) and further to the right (saltier). The high salinity of the California Current and the evidence presented that the high salinity was advected into the region point to new source waters for the California Current from 2017 to 2019. In particular, the formation of the salinity anomaly in the North Pacific Gyre suggests that increased Eastern North Pacific Central Water, which is relatively warmer and saltier, may have been in the California Current from 2017 to 2019.

With respect to biological impacts, new source water for the California Current from 2017 to 2019 may be important. Unusual water masses coming into the CCS may bring different biological and biogeochemical signatures to the local environment²⁸. In the CCS, zooplankton displacement volume has been found to be correlated with advection of the California Current^{29–31} (pp. 13–60), where displacement volume may be impacted by zooplankton body size and species composition. In light of recent sardine and anchovy abundance anomalies, reanalysis of fisheries models from 2005 to 2014 suggest that SST alone is not an adequate indicator of sardine biomass³². A plausible hypothesis is that different source water in 2017–2019 of the California Current brought water with different nutrient properties that supported a different plankton population. With respect to YOY rockfish, the relationship of higher abundance during cooler and fresher conditions¹⁹ appears to have held up in 2017–2019 with lower abundances observed in the warmer and saltier conditions².

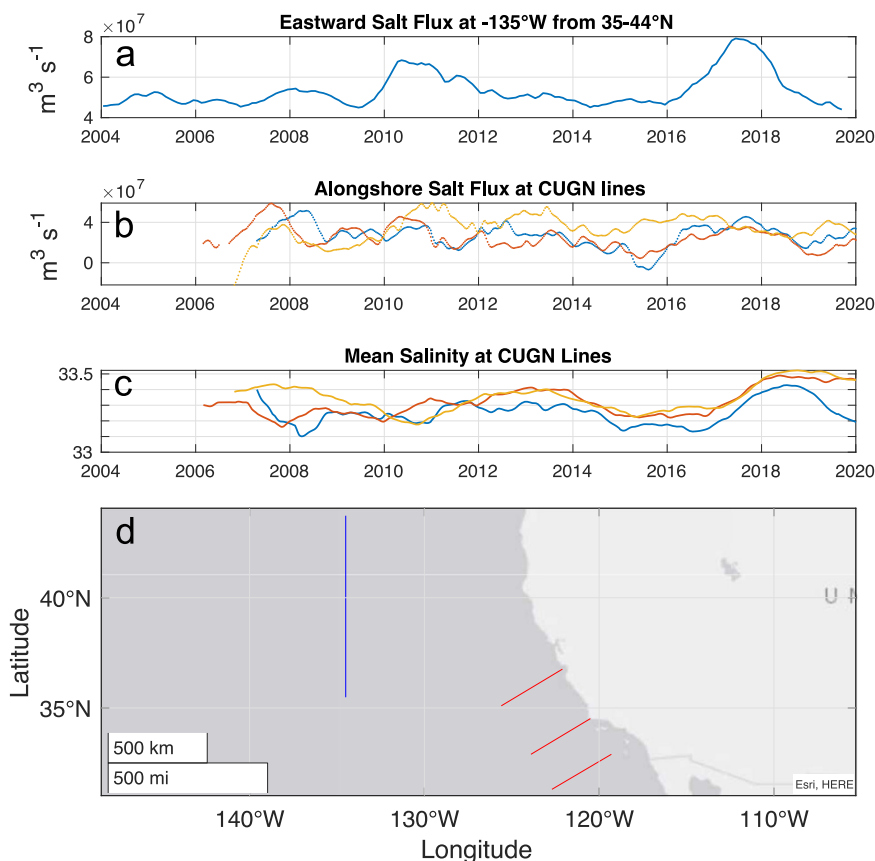


Fig. 5 Salt flux in the North Pacific and CCS. **a** Eastward salt flux integrated over the surface 100 m at 135°W from 35 to 44°N ($\text{m}^3 \text{s}^{-1}$). **b** Alongshore salt flux integrated over the surface 100 m at CUGN lines ($\text{m}^3 \text{s}^{-1}$). **c** Mean salinity averaged over the top 100 m at CUGN lines. For both **b**, **c** the across-shore extent of CUGN lines is the equivalent of CalCOFI stations 50–100, and Line 66.7 is plotted in blue, Line 80.0 in orange, and Line 90.0 in yellow. **d** Location of the North Pacific Current salt flux calculation (blue) and the three CUGN lines (red) on which salt flux and mean salinity were calculated.

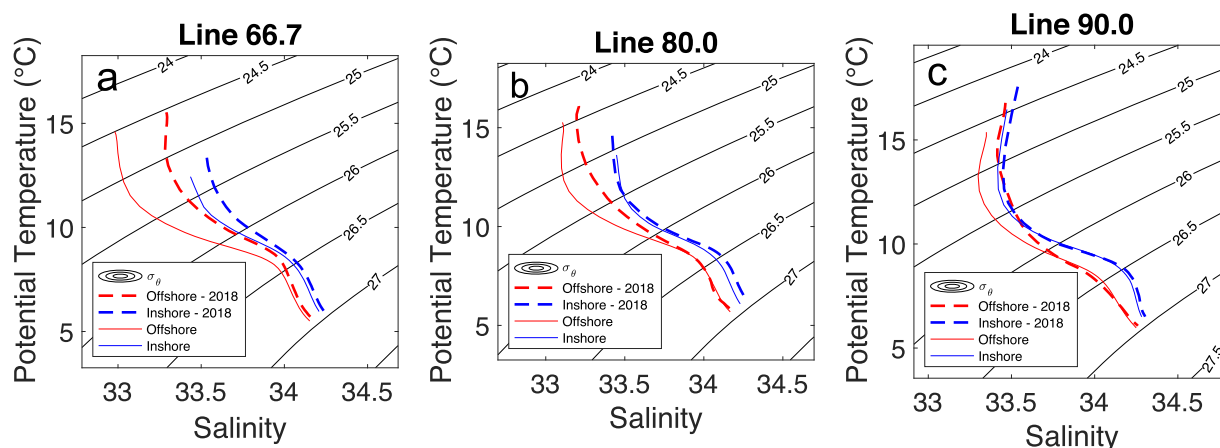


Fig. 6 T-S diagrams of 2018 compared to the mean. **a** Line 66.7, **b** Line 80.0, and **c** Line 90.0. Inshore is defined as 0–100 km and offshore as 200–400 km from shore. The mean is from 2007 to 2013 on Lines 80.0 and 90.0 and from 2008 to 2013 on Line 66.7.

Understanding source water changes may help with a more mechanistic understanding of forage fish population dynamics, which is needed to understand population fluctuations in a changing climate³³. Specifically, larval survival and recruitment may govern the population fluctuations of the species, and oceanic conditions may affect early life history survival. The mechanistic understanding of forage fish abundance is important as the CCS, combined with the other eastern boundary upwelling

systems represent around 20% of global marine fishing take over an area of around 1% of the global ocean³⁴.

The regional effects of climate variability may be more diverse than just increases in atmospheric or ocean temperature; here, it is shown that concomitant with anomalously high temperatures, a major regional current experienced a source water change and extreme salinity values. Experiencing both temperature anomalies and other effects such as source water changes concurrently may

have a large impact on the ocean ecosystem. Both salinity and temperature ocean observations should be sustained and further analyzed to better understand the marine physical environment as it changes.

Methods

Data came from three main sources: underwater gliders, shipboard hydrography, and Argo. Observations within 500 km of the coast were taken from gliders in the CUGN^{1,35}. CUGN gliders have been running off of the California coast since 2006 along three traditional CalCOFI hydrographic lines: Line 66.7 off of Monterey Bay, Line 80.0 off of Point Conception, and Line 90.0 from Dana Point (Fig. 1a). The gliders profile to 500 m completing a cycle from the surface to depth and back in 3 h and covering a horizontal distance of 3 km in that time. Gliders complete sections on the across-shore lines in roughly 2–3 weeks. A climatology of the CUGN data is available which includes the annual cycle and anomalies of measured variables temperature and salinity. Salinity in this manuscript is reported on the Practical Salinity Scale 1978, which is unitless. The annual cycle is computed from full years 2007–2013 on Lines 80.0 and 90.0 and 2008–2013 for Line 66.7 using a constant and three harmonics^{1,36}. Anomalies from this annual cycle are objectively mapped. Areas of the objective map where the ratio of error to signal variance is larger than 0.3 are masked out. The climatology is calculated in a gridded format with spacing of 10 days in time, 5 km in horizontal distance, and 10 m in depth with depth bins centered on 10, 20, and so on to 500 m. Analyses of temperature anomaly and salinity anomaly here used the CUGN climatology. The climatology also includes the alongshore geostrophic velocity calculated by referencing geostrophic shear to the glider's depth-average velocity³⁷. The calculation of alongshore salt flux used the geostrophic velocity and salinity of the CUGN climatology over the top 100 m and over the distance between CalCOFI stations 50–100 on each of the Lines 66.7, 80, and 90.

The CalCOFI hydrographic bottle-sample salinity and temperature from 1950 to 2019 was used to provide historical perspective. The CalCOFI program has been taking bottle samples of salinity and temperature since 1949 on Lines 80.0 and 90.0. The sampling pattern changed during the first few decades of CalCOFI, including years without cruises in the 1970s. A consistent sampling plan has been in place on Lines 80.0 and 90.0 since the 1980s with four cruises per year³¹ (pp. 8–11). CalCOFI has not maintained a consistent presence on Line 66.7. The CalCOFI program originally created a grid of offshore transects along the west coast of North America from Line 10 at the US–Canada border to Line 120 off Point Eugenia, Baja California, Mexico; however, only a core 66 station sampling survey spanning Lines 76.7–93.3 have been sampled for the entire time series (though with a period of less regular sampling in the 1970s–mid-1980s)³¹ (pp. 8–11). A CalCOFI time series was created using an annual average of data from Lines 80.0 and 90.0, stations 70, 80, 90, and 100 at 10 m depth. Data from years when both Line 80.0 and Line 90.0 had salinity data were included in the time series. CalCOFI anomalies were calculated as differences from the mean during 2007–2013, to be consistent with the mean used in the CUGN climatology. For comparison, CUGN climatology salinity and temperature anomalies at 10 m were averaged over the distance between stations 70 and 100 on Lines 80.0 and 90.0. Subsequently, a 365-day running mean was applied to the CUGN salinity and temperature anomaly time series.

The standard error of the mean was calculated for each year of the CalCOFI time series. The average standard error of all years for the salinity anomaly was 0.025, small compared to the interannual variations in the time series which were often 0.2. During a year with four cruises and data at all stations at 10 m, the CalCOFI sample size was $n = 32$. The average standard error of all years of the CUGN time series was 0.0024 where the sample size was $n = 3293$ climatology grid points per year. The standard error of the CUGN time series of salinity anomaly was less than that of CalCOFI, even considering autocorrelation in time and space of the CUGN profiles (reducing the effective CUGN sample size by a factor of 100 would make the standard errors comparable), so the standard error of CalCOFI was reported on the time series plot. Similarly, the standard error of the mean of the temperature anomalies was 0.26 °C for CalCOFI and 0.013 °C for CUGN, so only the CalCOFI standard error was reported on the plot. Importantly, with grid points every 5 km, the CUGN climatology is able to resolve mesoscale eddy variability, which can have a signature of 0.2 and 1 °C and greater in the CCS.

Salinity in the open ocean was from the R–G climatology of Argo data profiles^{24,38}. The R–G climatology calculates the monthly values of temperature and practical salinity on a $1^\circ \times 1^\circ$ grid with 58 pressure levels from 2.5 to 1975 db. The gridded product is produced by a weighted least-squares analysis that calculates the mean from the nearest 300 Argo observations, followed by objective analysis of the anomalies. An annual cycle for R–G salinity was calculated at every grid cell and pressure level using a constant and three harmonics for the full years 2007–2013, matching the method used to calculate the annual cycle for the CUGN climatology. Salinity anomaly was calculated as the difference from this annual cycle. Geopotential height, Z , was calculated by

$$Z = -\frac{1}{9.8} \int_{p_1}^{p_2} \frac{1}{\rho} dp \quad (1)$$

using the in-situ density, ρ , calculated from the R–G temperature and salinity and then integrating in pressure from $p_1 = 1975$ db to $p_2 = 2.5$ db³⁹. The

geostrophic velocity was calculated using

$$f(v_2 - v_1) = -9.8 \frac{\partial Z}{\partial x}, \quad (2)$$

$$f(u_2 - u_1) = 9.8 \frac{\partial Z}{\partial y}, \quad (3)$$

where the velocities u_1 and v_1 at 1975 db were assumed to be zero. The salt flux was calculated over the top 100 m using the R–G climatology salinity and the calculated geostrophic velocity.

Data availability

The CUGN glider data can be found online at <https://spraydata.ucsd.edu/projects/CUGN> (<https://doi.org/10.21238/S8SPRAY1618>), and the CUGN climatology is available at <https://spraydata.ucsd.edu/climCUGN> (<https://doi.org/10.21238/S8SPRAY7292>). The Argo data were collected and made freely available by the International Argo Program and the national programs that contribute to it (<http://www.argo.ucsd.edu>, <http://argo.jcommops.org>)³⁸. The Argo Program is part of the Global Ocean Observing System. The CalCOFI data can be found online at <https://calcofi.org/ccdata.html>.

Received: 22 September 2020; Accepted: 19 February 2021;

Published online: 19 March 2021

References

- Rudnick, D. L., Zaba, K. D., Todd, R. E. & Davis, R. E. A climatology of the California Current System from a network of underwater gliders. *Prog. Oceanogr.* **154**, 64–106 (2017).
- Thompson, A. R. et al. State of the California Current 2018–19: a novel anchovy regime and a new marine heat wave? *CalCOFI Rep.* **60**, 1–61 (2019).
- Zaba, K. D., Rudnick, D. L., Cornuelle, B. D., Gopalakrishnan, G. & Mazloff, M. R. Annual and interannual variability in the California Current System: comparison of an ocean state estimate with a network of underwater gliders. *J. Phys. Oceanogr.* **48**, 2965–2988 (2018).
- Zaba, K. D., Rudnick, D. L., Cornuelle, B., Gopalakrishnan, G. & Mazloff, M. Volume and heat budgets in the coastal California Current System: means, annual cycles and interannual anomalies of 2014–2016. *J. Phys. Oceanogr.* **50**, 1435–1453 (2020).
- Zaba, K. D. & Rudnick, D. L. The 2014–2015 warming anomaly in the Southern California Current System observed by underwater gliders. *Geophys. Res. Lett.* **43**, 1241–1248 (2016).
- Thompson, A. R. et al. State of the California Current 2017–18: still not quite normal in the North and getting interesting in the South. *CalCOFI Rep.* **59**, 1–66 (2018).
- Chavez, F. P., Ryan, J., Lluch-Cota, S. E. & Niquen, C. M. From anchovies to sardines and back: multidecadal change in the Pacific Ocean. *Science* **299**, 217–221 (2003).
- Jacobson, L. D. & MacCall, A. D. Erratum: Stock-recruitment models for Pacific sardine (*Sardinops sagax*). *Can. J. Fish. Aquat. Sci.* **52**, 2062–2062 (1995).
- Jacobson, L. D. & MacCall, A. D. Stock-recruitment models for Pacific sardine (*Sardinops sagax*). *Can. J. Fish. Aquat. Sci.* **52**, 566–577 (1995).
- Lindgren, M. & Checkley, D. M. Temperature dependence of Pacific sardine (*Sardinops sagax*) recruitment in the California Current Ecosystem revisited and revised. *Can. J. Fish. Aquat. Sci.* **70**, 245–252 (2012).
- Baumgartner, T. R., Soutar, A. & Ferreira-Bartrina, V. Reconstruction of the history of Pacific sardine and northern anchovy populations over the past two millennia from sediments of the Santa Barbara Basin. *CalCOFI Rep.* **33**, 24–40 (1992).
- McClatchie, S. Sardine biomass is poorly correlated with the Pacific decadal oscillation off California. *Geophys. Res. Lett.* **39**, <https://doi.org/10.1029/2012GL052140> (2012).
- McClatchie, S., Hendy, I. L., Thompson, A. R. & Watson, W. Collapse and recovery of forage fish populations prior to commercial exploitation. *Geophys. Res. Lett.* **44**, 1877–1885 (2017).
- Mantua, N. J., Hare, S. R., Zhang, Y., Wallace, J. M. & Francis, R. C. A Pacific interdecadal climate oscillation with impacts on Salmon production. *Bull. Am. Meteorol. Soc.* **78**, 1069–1080 (1997).
- Zwolinski, J. P., et al. Distribution, biomass and demography of the central-stock of Northern Anchovy during summer 2016, estimated from acoustic-trawl sampling. Report No. NOAA-TM-NMFS-SWFSC-572 (U.S. Department of Commerce, 2017).
- Zwolinski, J. P., Stierhoff, K. L. & Demer, D. A. Distribution, biomass, and demography of coastal pelagic fishes in the California Current Ecosystem during summer 2017 based on acoustic-trawl sampling. Report No. NMFS-SWFSC-610 (U.S. Department of Commerce, 2019).

17. Litzow, M. A. et al. Quantifying a novel climate through changes in PDO-climate and PDO-salmon relationships. *Geophys. Res. Lett.* **47**, e2020GL087972 (2020).
18. Muhling, B. A. et al. Predictability of species distributions deteriorates under novel environmental conditions in the California Current System. *Front. Mar. Sci.* <https://doi.org/10.3389/fmars.2020.00589> (2020).
19. Schroeder, I. D. et al. Source water variability as a driver of rockfish recruitment in the California Current Ecosystem: implications for climate change and fisheries management. *Can. J. Fish. Aquat. Sci.* **76**, 950–960 (2019).
20. Lynn, R. J. & Bograd, S. J. Dynamic evolution of the 1997–1999 El Niño–La Niña cycle in the southern California Current System. *Prog. Oceanogr.* **54**, 59–75 (2002).
21. Bograd, S. J. & Lynn, R. J. Physical-biological coupling in the California Current during the 1997–99 El Niño–La Niña Cycle. *Geophys. Res. Lett.* **28**, 275–278 (2001).
22. Bond, N. A., Cronin, M. F., Freeland, H. & Mantua, N. Causes and impacts of the 2014 warm anomaly in the NE Pacific. *Geophys. Res. Lett.* **42**, 3414–3420 (2015).
23. Amaya, D. J., Miller, A. J., Xie, S.-P. & Kosaka, Y. Physical drivers of the summer 2019 North Pacific marine heatwave. *Nat. Commun.* **11**, 1903 (2020).
24. Roemmich, D. & Gilson, J. The 2004–2008 mean and annual cycle of temperature, salinity, and steric height in the global ocean from the Argo Program. *Prog. Oceanogr.* **82**, 81–100 (2009).
25. Di Lorenzo, E. & Mantua, N. Multi-year persistence of the 2014/15 North Pacific marine heatwave. *Nat. Clim. Change* **6**, 1042–1047 (2016).
26. Di Lorenzo, E. et al. North Pacific gyre oscillation links ocean climate and ecosystem change. *Geophys. Res. Lett.* **35**, <https://doi.org/10.1029/2007gl032838> (2008).
27. Litzow, M. A. et al. The changing physical and ecological meanings of North Pacific Ocean climate indices. *Proc. Natl Acad. Sci. USA* **117**, 7665–7671 (2020).
28. Bograd, S. J., Schroeder, I. D. & Jacox, M. G. A water mass history of the Southern California current system. *Geophys. Res. Lett.* **46**, 6690–6698 (2019).
29. Bernal, P. A. & McGowan, J. Advection and upwelling in the California current. In *Coastal Upwelling*. Vol. 1 (ed. Francis A. Richards) 381–399 (American Geophysical Union, Washington DC, 1981).
30. Chelton, D. B. Interannual variability of the California Current-physical factors. *California Cooperative Oceanic Fisheries Investigations Rep.* **22**, 130–148 (1981).
31. McClatchie, S. *Regional Fisheries Oceanography of the California Current System: The CalCOFI Program*. 8–11, 13–60 (Springer, Netherlands, 2014).
32. Zwolinski, J. P. & Demer, D. A. Re-evaluation of the environmental dependence of Pacific sardine recruitment. *Fish. Res.* **216**, 120–125 (2019).
33. Checkley, D. M. Jr., Asch, R. G. & Rykaczewski, R. R. Climate, anchovy, and sardine. *Annu. Rev. Mar. Sci.* **9**, 469–493 (2017).
34. Chavez, F. P. & Messié, M. A comparison of eastern boundary upwelling ecosystems. *Prog. Oceanogr.* **83**, 80–96 (2009).
35. Rudnick, D. L. California Underwater Glider Network. Scripps Institution of Oceanography, Instrument Development Group. <https://doi.org/10.21238/S8SPRAY1618> (2016).
36. Rudnick, D. L., Zaba, K. D., Todd, R. E. & Davis, R. E. A climatology using data from the California Underwater Glider Network. Scripps Institution of Oceanography, Instrument Development Group. <https://doi.org/10.21238/S8SPRAY7292> (2017).
37. Rudnick, D. L., Sherman, J. T. & Wu, A. P. Depth-average velocity from spray underwater gliders. *J. Atmos. Ocean. Technol.* **35**, 1665–1673 (2018).
38. Argo. Argo float data and metadata from Global Data Assembly Centre (Argo GDAC). <https://doi.org/10.17882/42182> (2000).
39. Talley, L. D., Pickard, G. L., Emery, W. J. & Swift, J. H. *Descriptive Physical Oceanography: An Introduction*. 6th edn (Elsevier, 2011).

Acknowledgements

We gratefully acknowledge the support of the National Oceanographic and Atmospheric Administration Global Ocean Monitoring and Observation Program (NA15OAR4320071) and Integrated Ocean Observing System (NA16NOS012022). In addition, we are grateful for the DOD NDSEG fellowship which supported A.S.R. The Instrument Development Group at Scripps Institution of Oceanography is responsible for operations of Spray gliders in the CUGN. In particular, we thank Jeff Sherman, Ben Reineman, Evan Goodwin, Derek Vana, and Kyle Grindley.

Author contributions

A.S.R. wrote the manuscript, performed the analysis, and generated all figures. D.L.R. developed the original idea for the manuscript, provided guidance in analysis, and edited and revised the manuscript.

Competing interests

The authors declare no competing interests.

Additional information

Supplementary information The online version contains supplementary material available at <https://doi.org/10.1038/s43247-021-00131-9>.

Correspondence and requests for materials should be addressed to A.S.R.

Peer review information Primary handling editor: Joe Aslin.

Reprints and permission information is available at <http://www.nature.com/reprints>

Publisher's note Springer Nature remains neutral with regard to jurisdictional claims in published maps and institutional affiliations.



Open Access This article is licensed under a Creative Commons Attribution 4.0 International License, which permits use, sharing, adaptation, distribution and reproduction in any medium or format, as long as you give appropriate credit to the original author(s) and the source, provide a link to the Creative Commons license, and indicate if changes were made. The images or other third party material in this article are included in the article's Creative Commons license, unless indicated otherwise in a credit line to the material. If material is not included in the article's Creative Commons license and your intended use is not permitted by statutory regulation or exceeds the permitted use, you will need to obtain permission directly from the copyright holder. To view a copy of this license, visit <http://creativecommons.org/licenses/by/4.0/>.

© The Author(s) 2021